JOURNAL OF NEUROPHYSIOLOGY
Vol. 76, No. 5, November 1996. *Printed in U.S.A.*

Origins of the Power Law Relation Between Movement Velocity and Curvature: Modeling the Effects of Muscle Mechanics and Limb Dynamics

PAUL L. GRIBBLE AND DAVID J. OSTRY
McGill University, Montreal, Quebec H3A 1B1, Canada

SUMMARY AND CONCLUSIONS

1. When subjects trace patterns such as ellipses, the instantaneous velocity of movements is related to the instantaneous curvature of the trajectories according to a power law—movements tend to slow down when curvature is high and speed up when curvature is low. It has been proposed that this relationship is centrally planned.

2. The arm's muscle properties and dynamics can significantly affect kinematics. Even under isometric conditions, muscle mechanical properties can affect the development of muscle forces and torques. Without a model that accounts for these effects, it is difficult to distinguish between kinematic patterns that are attributable to central control and patterns that arise because of dynamics and muscle properties and are not represented in the underlying control signals.

3. In this paper we address the nature of the control signals that underlie movements that obey the power law. We use a numerical simulation of arm movement control based on the λ version of the equilibrium point hypothesis. We demonstrate that simulated elliptical and circular movements, and elliptical force trajectories generated under isometric conditions, obey the power law even though there was no relation between curvature and speed in the modeled control signals.

4. We suggest that limb dynamics and muscle mechanics—specifically, the springlike properties of muscles—can contribute significantly to the emergence of the power law relationship in kinematics. Thus, without a model that accounts for these effects, care must be taken when making inferences about the nature of neural control.

INTRODUCTION

It has been reported in a number of empirical studies (Lacquaniti et al. 1983; Pollick and Sapiro 1996; Viviani and Cenzato 1985; Viviani and Flash 1995; Viviani and Schneider 1991; Viviani and Stucchi 1992) that when subjects trace patterns such as ellipses, there is a reliable coupling between the curvature and the speed of movement—movements are slower in more curved parts of the trajectory. It has been shown that these movements obey the following power law

$$V = K(R^*)^{\beta} \tag{1}$$

where

$$R^* = \left(\frac{R}{1 + \alpha R}\right) \tag{2}$$

and where V is hand tangential velocity and R is the radius of curvature of the movement (see *Eqs. 8* and *9*, below). The parameter K is a "velocity gain factor" that is related to movement speed and that has been shown to be useful in segmenting complex movements (see Viviani and Cenzato 1985).

The value of α is inversely related to the average velocity of the movement (see Viviani and Stucchi 1992), and β represents the slope of the logarithmic form of the power law relation. If we take the logarithm of both sides, the relation becomes

$$\log V = \log K + \beta \log R^* \tag{3}$$

Thus log V and log R^* are linearly related with a slope of β and an intercept of log K.

The value of β has been estimated under a variety of experimental conditions. These include the production of complex shapes of various sizes and at different movement rates (Pollick and Sapiro 1996; Viviani and Cenzato 1985; Viviani and Flash 1995), and tracings of ellipses and lemniscates (figure 8s) under isometric conditions (Massey et al. 1992). The power law relationship has been shown to hold for planar movements, regardless of the orientation of the plane.

In each of these situations, the estimates of β have been found to be consistently close to one third. Because of this result, the relationship has been termed the "one third power law." (Note that when the relation between curvature and velocity is specified in angular as opposed to Cartesian coordinates, estimates of β are typically close to 2/3, and in this context the relationship is referred to as the "2/3 power law".) In the present paper we use a Cartesian coordinate system and refer to the empirical relationship between curvature and velocity as the one third power law.

It has been suggested that the relationship between radius of curvature and hand velocity does not arise as a result of muscle properties and limb dynamics (Viviani and Cenzato 1985), but rather reflects a rule used by the nervous system in motion planning (Viviani and Flash 1995). The demonstration that the power law holds under isometric conditions (Massey et al. 1992) is consistent with the idea that it may not be due to the mechanical properties of the arm. The demonstration by Schwartz (1994) that hand area motor cortical activity obeys the power law supports the view that this relationship may be centrally planned.

The power law may indeed be centrally planned. However, to identify characteristics of movements that are speci-

fied centrally, it is necessary to take account of the contribution of the mechanical and dynamic properties of the arm, because these can significantly affect the kinematics. Even under isometric conditions, muscle properties can affect the development of muscle forces and torques. Thus, without accounting for these factors specifically, it is difficult to separate those aspects of movements that reflect properties of central control from those that arise from properties of the physical plant and are not represented in neural control signals.

The goal of the present paper is to explore the control of drawing movements that obey the power law, in the context of simulations of two-joint arm movement based on the equilibrium point hypothesis. We suggest that muscle properties can contribute significantly to the emergence of the power law, both in the case of limb movements and in the case of force-space trajectories under isometric conditions. Thus, before drawing inferences about the nature of central neural control on the basis of kinematic observables, these limb and muscle mechanical factors must be accounted for.

Arm model

We present a brief description of a model of planar two-joint arm movement. We direct the reader to Laboissière et al. (1996) for a more detailed presentation of our approach, in the context of a model of human jaw and hyoid motion.

The arm model is implemented as a computer simulation and has two kinematic degrees of freedom: rotation at the shoulder joint and at the elbow joint, in the horizontal plane. Six muscles are included in the model—pectoralis and deltoid (single joint shoulder muscles), biceps long head and triceps lateral head (single joint elbow muscles), and biceps short head and triceps long head, which span the shoulder and elbow (see Fig. 1). Muscle moment arms are calculated on the basis of musculoskeletal geometry, and thus vary as a function of joint angle. Consistent with empirical measurements, the simulated moment arms of flexor muscles vary between 2 and 4 cm over the full range of shoulder and elbow angles, and moment arms of extensor muscles are effectively constant—2 cm at the shoulder and 2.5 cm at the elbow. Musculoskeletal geometry has been estimated from anatomic sources (An et al. 1989a,b; Winters and Woo 1990). The equations of motion relating joint torques to accelerations were obtained with the use of the Lagrangian approach (see Hollerbach and Flash 1982).

Control signals in the model are based on the equilibrium point hypothesis (λ version) (Feldman 1986; Feldman et al. 1990). According to the λ model, neural control signals specify muscle threshold lengths (λs) for motoneuron (MN) recruitment (Feldman et al. 1990). Muscle activation, A, is proportional to the difference between the current muscle length, l, and the centrally specified threshold length for MN recruitment, λ, as well as on the rate of muscle length change, $\dot{l}$

$$A = [l - \lambda + \mu\dot{l}]^+ \tag{4}$$

where

$$[x]^+ = \begin{cases} x, & \text{if } x > 0 \\ 0, & \text{if } x \leq 0 \end{cases} \tag{5}$$

The parameter μ specifies the dependence of the muscle's threshold length on velocity and provides damping due to proprioceptive feedback. μ is set at 0.05 s, and is constant throughout each of the simulated movements. Damping due to intrinsic muscle properties such as the dependence of force on the velocity of muscle lengthening or shortening is also included in the model (see Fig. 1).

A reflex delay, d, of 30 ms has been used for all muscles. This value was estimated from delays observed in unloading responses in human arm muscles (Houk and Rymer 1981). Thus, taking into account time-varying central neural commands $\lambda(t)$ and a reflex delay d, the muscle activation $A(t)$ is

$$A(t) = [l(t - d) - \lambda(t) + \mu(t)\dot{l}(t - d)]^+ \tag{6}$$

Changes to λ and thus to muscle activation are associated with MN recruitment and changes in MN firing rates. The resulting active muscle force, $\tilde{M}$, is approximated with the use of an exponential function of the form

$$\tilde{M} = \rho[\exp(cA) - 1] \tag{7}$$

where c is a form parameter that is estimated on the basis of empirical data and is the same for all muscles. As in Laboissière et al. 1996, a value of $c = 0.112$ mm^{-1} is used. Values of ρ are scaled in proportion to estimates of the modeled muscles' physiological cross-sectional areas that were obtained from Winters and Woo (1990). The following values of ρ are used: pectoralis, 16.8 N, deltoid, 12.6 N, biceps long head, 19.0 N, triceps lateral head, 12.0 N, biceps short head, 4.2 N, and triceps long head, 13.4 N. Note that the exponential form of the dependence of force on muscle length is consistent with the size principle for MN recruitment (Henneman et al. 1965). As the difference between the actual and threshold muscle length increases, progressively larger motor units are recruited and larger increments in force are observed.

The muscle model also includes the dependence of muscle force on the velocity of muscle lengthening or shortening (Joyce and Rack 1969), the graded development of force over time due to calcium-dependent muscle kinetics (Huxley 1957), and the passive elastic stiffness of muscle (Feldman and Orlovsky 1972). The force-velocity relation was obtained by fitting data for cat soleus muscle (obtained from Joyce and Rack 1969) with a sigmoidal function that accounts for the dependence of force on velocity during both muscle shortening and lengthening. The graded development of muscle force was modeled with the use of a second-order, low-pass filtering of the steady-state muscle force, $\tilde{M}$ (see *Eq. 7*). The filter is critically damped and has a time constant of 25 ms, which leads to an asymptotic response to a step input in ~150 ms. The passive elastic stiffness of muscle was assumed to vary linearly with muscle length, and to summate with active muscle force. Stiffness values for each muscle were obtained by assuming that passive stiffness scales linearly with physiological cross-sectional area. Passive muscle stiffness estimates are as follows: pectoralis, 291.5 N/m, deltoid, 218.6 N/m, biceps long head, 329.7 N/m, triceps lateral head, 208.2 N/m, biceps short head, 72.9 N/m, and triceps long head, 232.5 N/m (see Fig. 1 for a schematic and Laboissière et al. 1996 for further details).

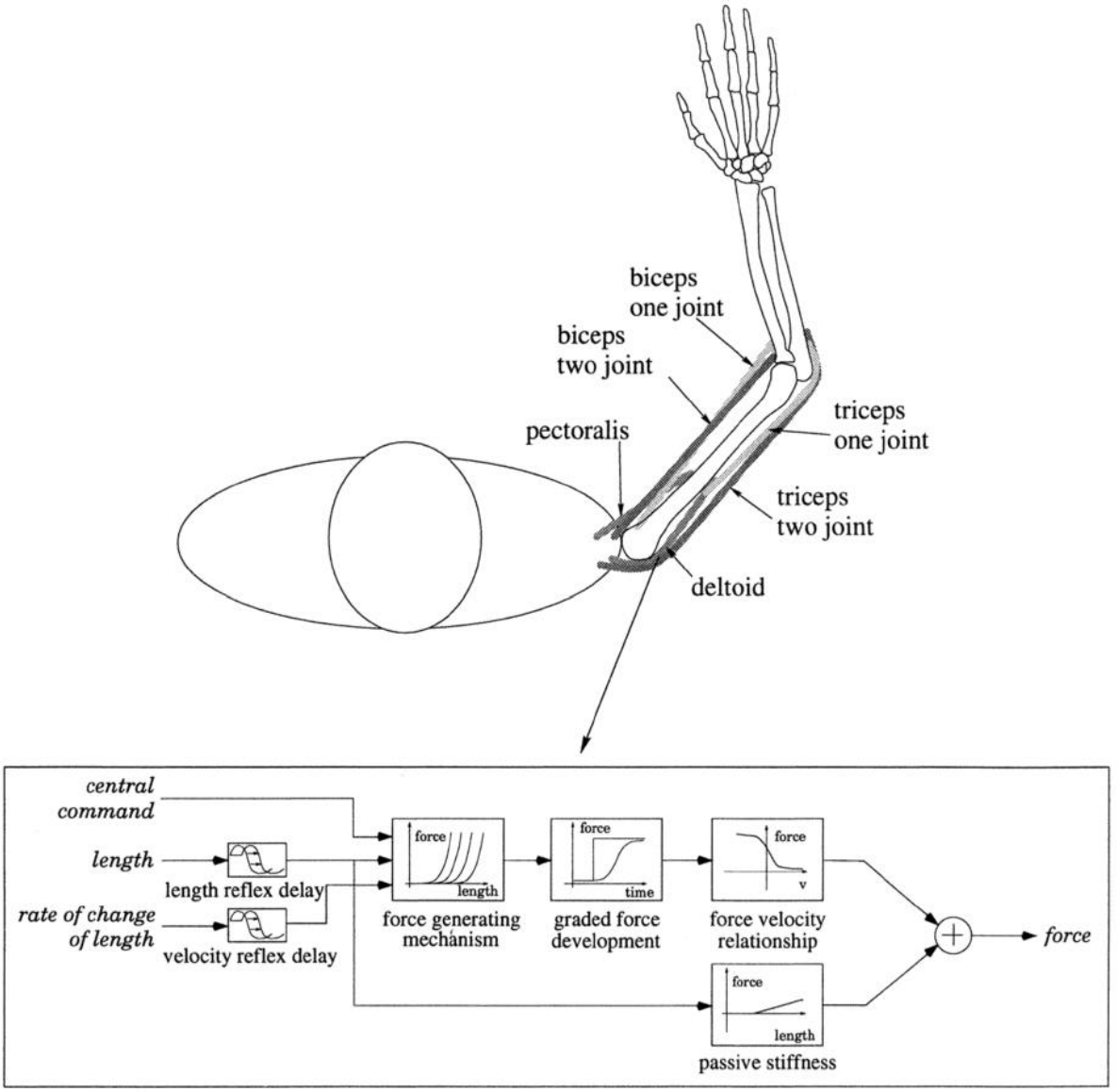

FIG. 1. Arm model. Six muscles are modeled, including 2 muscles that span both joints. *Inset*: schematic of the muscle model that includes the dependence of force on muscle length and velocity, the graded development of force over time, the passive elastic stiffness of muscle, and length and velocity afferent feedback with reflex delays.

According to the equilibrium point hypothesis, movements arise from shifts in the equilibrium position of the limb. The equilibrium position is a consequence of the interaction of central neural commands (the 6 muscle λs), reflex mechanisms, muscle properties, and loads. By changing the values of λs over time, the nervous system can shift the position of the limb. As the λs change value, forces develop in each muscle in proportion to the difference between the muscle's current length and its threshold length. These forces drive the limb toward a new equilibrium position. In this way the model proposes that the nervous system may produce limb movements by specifying the appropriate time-varying sequence of λ changes.

Because the number of muscles (6) exceeds the kinematic degrees of freedom (2) in the model, there are an infinite set of λs associated with any given posture of the limb. These different λ combinations define different levels of total force, that is, different levels of cocontraction for a given limb configuration. In the simulations presented here, movements are defined as a sequence of postures, generated with the use of a series of via points. λs are shifted at a constant rate from a set of λs associated with an initial posture of the limb, to the nearest point, in λ space, associated with the next position in the sequence. In other words, we have assumed that to generate movements between via points, the shortest distance in λ space is selected. This is equivalent to minimizing the total change in central commands (see Laboissière et al. 1996 for details). As a control, other methods of choosing λs were tested, including minimizing the total change in muscle forces and minimizing the total change in joint torques—these methods generated results similar to those reported below.

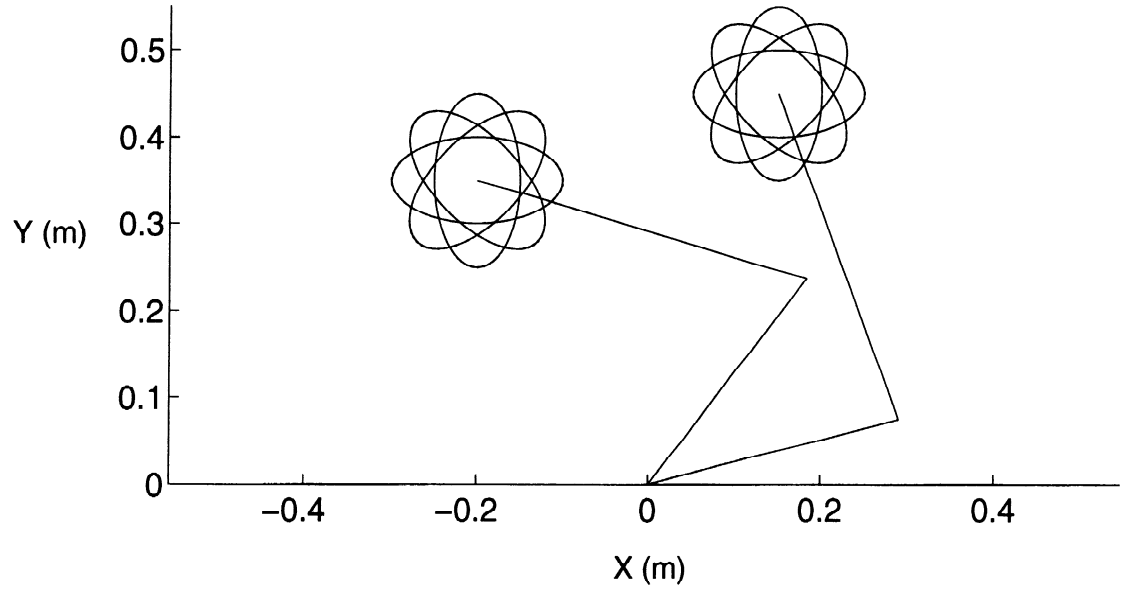

FIG. 2. Arm configurations and simulated equilibrium trajectories are shown to scale for the 2 workspace positions we tested. Coordinates of the shoulder are (0,0).

METHODS

To explore the nature of the control signals that underlie movements that obey the power law, we examined simulations of elliptical and circular movements as well as elliptical force-space trajectories under isometric conditions. In each case, we examined the effects of using control signals in which there was no relationship between curvature and speed—that is, in which the power law was not represented.

We simulated elliptical tracings with the use of elliptical equilibrium hand paths constructed so that the tangential velocity was held constant over time. Equilibrium paths were generated as a series of 36 via points equally spaced in time and equally spaced along the circumference of an ellipse in hand space. The major axis of the ellipse was 20 cm long and the minor axis was 10 cm long. The space between via points was 1.38 cm.

Movements were simulated in two areas of the arm's workspace (see Fig. 2): the first was located 20 cm to the left of the shoulder and 35 cm forward and the second was located 15 cm to the right of the shoulder and 45 cm forward. For each of the two workspace areas we used elliptical equilibrium paths whose major axes were oriented in four directions: 0, 45, 90, and 135° from the frontal plane. To investigate the effects of different movement rates, the hand equilibrium positions were shifted at two rates comparable with those used by Viviani and Flash (1995): 0.6 and 0.8 revolutions per second. In all 16 conditions (2 workspace positions × 2 rates × 4 ellipse orientations), movements were simulated for 10 s, which was sufficient to trace the curves several times.

We also generated simulations with the use of a circular equilibrium path, which had both constant tangential velocity and constant radius of curvature over time. The circular path was constructed with the use of 36 via points, had a diameter of 10 cm, and was tested in a single workspace location, 20 cm to the left of the shoulder and 35 cm forward. The space between via points was 0.87 cm. Two movement speeds were used: 0.6 and 0.8 revolutions per second. Again, the movements were simulated for 10 s.

Finally, we examined simulations generated under isometric conditions. The simulated limb was fixed in place with the hand at the center of an elliptical equilibrium path whose long axis was parallel to the frontal plane. The equilibrium path had constant tangential velocity. Two rates of equilibrium position shift (1.5 and 2.0 Hz) were simulated in a single workspace area. The hand was located 40 cm directly in front of the shoulder (comparable conditions are reported in Massey et al. 1992). Simulated force vectors generated at the hand as a result of the elliptical constant rate equilibrium position shift were calculated and plotted in X-Y space, and were represented as two-dimensional force-space trajectories.

RESULTS

To investigate the extent to which the simulated movements obeyed the power law, the instantaneous tangential velocities, V, and the instantaneous radii of curvature, R, of the simulated trajectories were calculated with the use of the following equations (Viviani and Stucchi 1992)

$$V = \sqrt{\dot{X}^2 + \dot{Y}^2} \tag{8}$$

and

$$R = \frac{(\dot{X}^2 + \dot{Y}^2)^{3/2}}{|\dot{X}\ddot{Y} - \ddot{X}\dot{Y}|} \tag{9}$$

Velocities ($\dot{X}$, $\dot{Y}$) and accelerations ($\ddot{X}$, $\ddot{Y}$) of simulated hand positions were calculated numerically.

Figure 3, *top*, shows simulated elliptical paths produced at a rate of 0.6 and 0.8 revolutions per second in the left area of the workspace. All four orientations are shown. The hand paths are smooth and elliptical in shape. The variability that is present in the simulated paths is due to changes in the levels of total muscle force from cycle to cycle that arise as a result of using commands that minimize the total λ change from one via point to the next. Figure 3, *middle*, shows the simulated radius of curvature, R, and tangential velocity, V, plotted against time for a single simulation. The correlation between simulated curvature and velocity is apparent. Figure 3, *bottom*, shows the logarithm of tangential velocity, V, plotted against the logarithm of radius of curvature, R^* (see *Eq. 2*), for two simulated movements. The dotted lines show the relation for ellipses simulated in the left area of the workspace at a rate of 0.6 Hz, with the major axis oriented parallel to the frontal plane. The solid lines display the relation for ellipses simulated

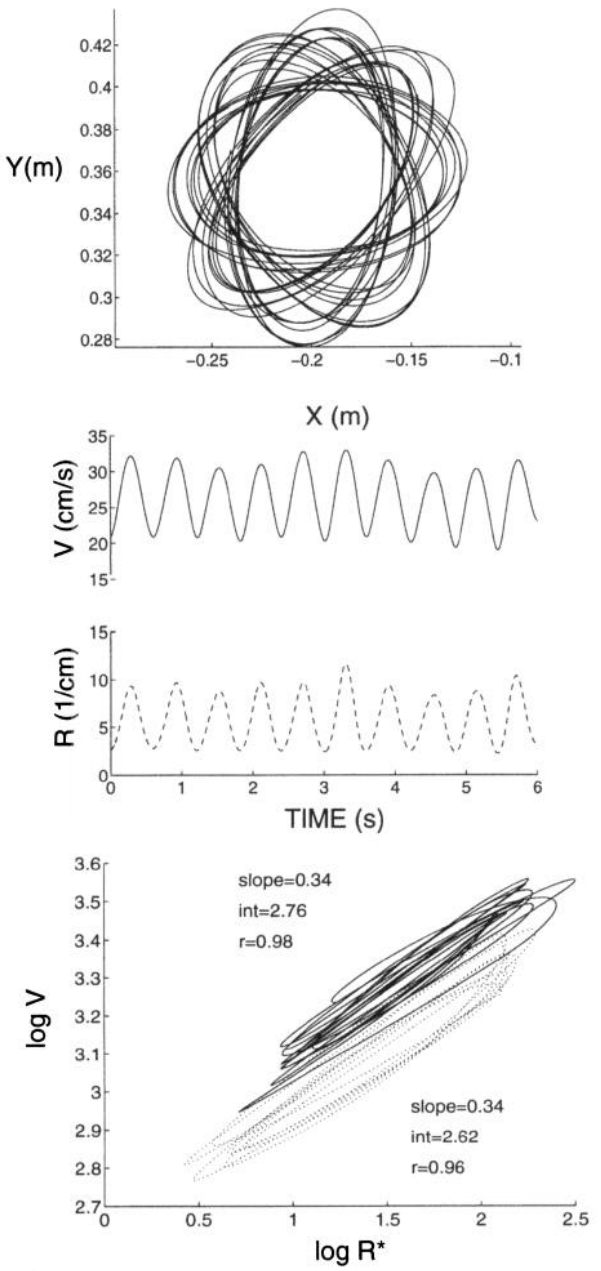

FIG. 3. Predicted elliptical movements with the use of simulated control signals with constant tangential velocity. *Top*: simulated hand paths for elliptical tracings in the left area of the workspace, in 4 orientations. Ellipses associated with slower movements are larger. *Middle*: tangential velocity, V, and radius of curvature, R, plotted against time for a single simulation. *Bottom*: log V plotted against log R^* for 2 simulated elliptical movements, both oriented with the long axis of the ellipse parallel to the frontal plane. Dotted lines: 0.6-Hz tracings in the left area of the workspace. Solid lines: 0.8-Hz tracings in the right area of the workspace.

in the right area of the workspace at a rate of 0.8 Hz, with the major axis also oriented parallel to the frontal plane. Note that two different areas of the workspace are shown to illustrate the generality of the findings (similar results were also obtained when the simulations were performed in other parts of the workspace). The parameter α in *Eq. 2* was set to 0.01 for movements made at 0.8 Hz and to 0.05 for movements made at 0.6 Hz (comparable values of α were reported in Viviani and Stucchi 1992).

In accordance with the power law, the relations are highly linear, and the slopes, β, are both close to one third (β = 0.34 for both the 0.8-Hz and the 0.6-Hz simulations). As the movement speed is increased, the slope of the relation remains about the same, but the intercept increases. For the 0.6-Hz simulations, log K = 2.62, and for the 0.8 Hz simulations, log K = 2.76. Comparable values of log K are reported in empirical studies, and similar increases in the values of log K are associated with faster movement speeds (Viviani and Cenzato 1985; Viviani and Flash 1995).

A quantitative analysis of the elliptical movement simulations was carried out by computing the linear regression of log V against log R^* for each of the 16 simulated conditions. Table 1 displays β and log K values (see *Eq. 1* and *2*) for each of the 16 simulated ellipses, as well as correlation coefficients, ρ, for each regression.

It is clear from Table 1 that the correlation coefficients, ρ, for the regressions of log V on log R^*, computed over the course of the movements, are all very close to 1.00, indicating that a reliable linear relationship is present (0.95 $\pm$ 0.03, mean $\pm$ SD). In addition, β, the slope of the relation between log V and log R^*, is close to one third for simulated tracings in both areas of the workspace, for all four orientations, and at both rates (0.33 $\pm$ 0.02, mean $\pm$ SD). In addition, the predicted values of log K shown in Table 1 increase as the rate of the simulated movements increases. For simulated tracings at a rate of 0.6 Hz, the mean value of log K is 2.64 and the SD is 0.04, and for tracings at a rate of 0.8 Hz, the mean value of log K is 2.75, and the SD is 0.03. Once again, similar values are reported in empirical studies (Viviani and Cenzato 1985; Viviani and Flash 1995).

Figure 4, *top,* shows simulated circular tracings at two movement rates (0.6 and 0.8 Hz). The simulated movements are generally smooth, and they follow a relatively circular path. Deviations from a perfectly circular path arise because of muscle mechanics and the dynamics of the moving limb. Variability also arises, as in the case of the elliptical trajectories, because of changes in the distribution of muscle forces that occur as a result of using commands that minimize the total λ change between via points. Figure 4, *middle,* shows simulated tangential velocity, V, and radius of curvature,

TABLE 1. *Analysis of simulated hand paths*

Location/ Orientation	Rate = 0.6 Hz			Rate = 0.8 Hz		
	β	log K	ρ	β	log K	ρ
Left side						
0°	0.331	2.62	0.945	0.321	2.77	0.967
45°	0.312	2.68	0.946	0.336	2.76	0.977
90°	0.343	2.61	0.975	0.335	2.75	0.972
135°	0.336	2.61	0.956	0.337	2.70	0.978
Right side						
0°	0.339	2.62	0.964	0.319	2.77	0.983
45°	0.266	2.72	0.900	0.289	2.78	0.955
90°	0.314	2.65	0.880	0.333	2.76	0.957
135°	0.362	2.63	0.931	0.342	2.74	0.982

β and log K values are shown (see *Eqs. 1* and *2*) for each of the 16 simulated hand paths, as well as correlation coefficients. (ρ) for each linear regression of log V against log R^*. Simulations were generated using elliptical equilibrium trajectories oriented in 4 directions, traced at 2 rates, and drawn in 2 areas of the arm's workspace.

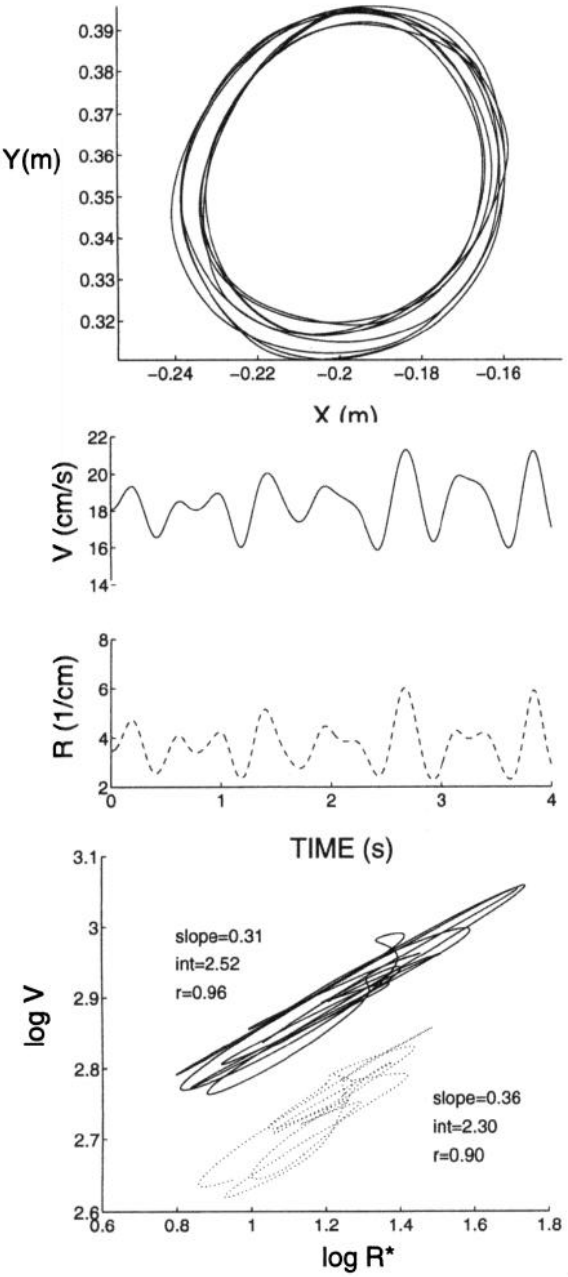

FIG. 4. Simulated circular movements generated with the use of control signals with constant radius of curvature and constant tangential velocity. *Top*: simulated circular hand paths for movements in the left area of the workspace, at two rates—0.6 and 0.8 Hz. The larger circles are for the slower movements. *Middle*: tangential velocity, V, and radius of curvature, R, plotted against time for the 0.8-Hz simulation. *Bottom*: log V plotted against log R^* for the 2 simulations displayed at *top*.

R, plotted against time. A consistent relationship between curvature and velocity may be seen. Figure 4, *bottom,* shows that the simulated circular tracings conform to the power law. The dotted lines show the relation between log V and log R^* for circles simulated at a rate of 0.6 Hz, and the solid lines show the relation for circles simulated at a rate of 0.8 Hz. As was the case for the elliptical simulations, the relation between log V and log R^* is linear, with a slope close to one third ($\beta = 0.36$ for the 0.6-Hz simulation, and $\beta = 0.31$ for the 0.8-Hz simulation). The correlation coefficients for the regression are 0.90 for the 0.6-Hz circle and 0.96 for the 0.8-Hz circle. In addition, as in the case of the elliptical simulations, when the rate of movement is increased, the slope of the relation remains about the same, but the intercept, log K, increases. For the 0.6-Hz circles, log K is 2.30, and for the 0.8-Hz circles, log K is 2.52.

Figure 5, *top,* displays a single simulated elliptical tracing, produced at a rate of 2.0 Hz, under isometric conditions. Figure 5, *middle,* shows the tangential velocity, V, and the

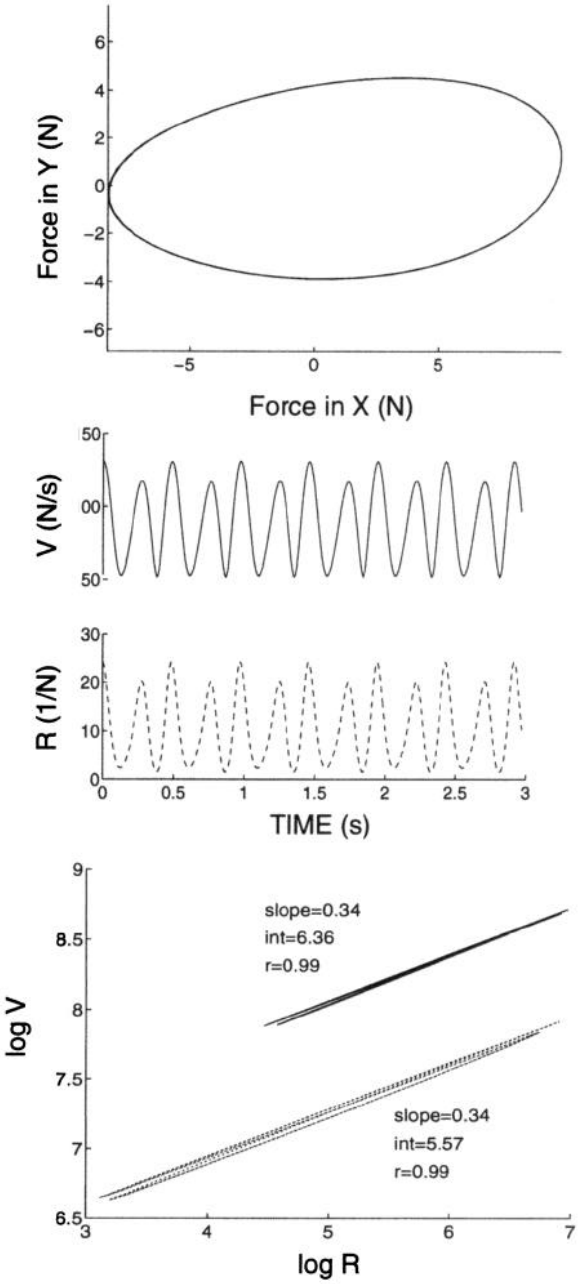

FIG. 5. Simulated elliptical force trajectories under isometric conditions. The hand was fixed in the center of the workspace, and forces at the hand were generated with the use of simulated control signals with constant tangential velocity. *Top*: simulated force trajectory at the hand generated by an elliptical equilibrium path shifted at a constant rate of 2.0 Hz. *Middle*: tangential velocity, V, and radius of curvature, R, plotted against time. *Bottom*: log V plotted against log R for elliptical force trajectories generated with the use of 2.0- and 1.5-Hz equilibrium shifts.

radius of curvature, R, of this force trajectory plotted against time. A correlation between curvature and speed is again evident. Figure 5, *bottom,* shows that the two isometric simulations conform to the power law. The dotted lines give the simulated relation between log V and log R for a 1.5-Hz elliptical force trajectory. The solid lines show the relation for the 2.0-Hz simulation that is presented at the *top* and *middle.*

The relationship between the logarithms of curvature and velocity is linear for both force trajectories; the slopes are both close to one third ($\beta = 0.34$ for both the 1.5- and 2.0-Hz simulations). As was the case with the elliptical and circular movement paths, the effect of increasing movement rate was to increase the value of the intercept, log K, without changing the slope of the relation. For the 1.5-Hz isometric ellipses, log $K = 5.57$, and for the 2.0-Hz ellipses, log $K = 6.36$. Note that the values of log K are different than those in movement simulations because in the isometric simulations curvature and velocity are expressed in units of force.

DISCUSSION

In this paper we demonstrate that simulated elliptical tracing movements obey the power law, even when the modeled control signals have constant tangential velocity—in other words, the power law relation is observed in kinematics even when no relation between curvature and velocity exists in the modeled control signals. We also show that simulated elliptical movements obey the power law in different areas of the limb's workspace, and that the power law relation is unaffected by varying the orientation of the simulated ellipses. In addition, we show, in agreement with previous empirical results (Viviani and Cenzato 1985; Viviani and Flash 1995), that increasing the rate of the simulated movements affects the intercept of the relationship between the logarithms of curvature and velocity, but does not affect the slope, which remains relatively close to one-third.

We also show that simulated circular movements, generated by control signals that have both constant tangential velocity and constant radius of curvature, also obey the power law. Last, we show that simulated elliptical force-space trajectories generated under isometric conditions likewise conform to the power law, even though the power law relation was not present at the level of the modeled control signals, which were constructed to have constant tangential velocity.

The finding that the power law can be predicted with the use of modeled control signals in which there is no relation between movement speed and curvature suggests that muscle properties and dynamics can play a significant role in the emergence of this relationship. The power law arises in these simulations because of forces developed due to equilibrium shifts. As the equilibrium position of the limb travels about an elliptical orbit, forces develop in muscles in proportion to the difference between the actual and equilibrium positions of the limb. As the equilibrium position reaches its maximum extent and changes direction, muscle forces are developed that oppose the actual movement, decelerating the limb when curvature is high.

The power law emerges in the simulations of circular movements for similar reasons. Because of the dynamics of the moving limb, interaction torques that affect the limb's trajectory result in departures from a circular path. As in the case of elliptical trajectories, when the equilibrium changes direction, forces develop in the opposite direction that decelerate the limb in the regions of greatest curvature. Under isometric conditions, the development of muscle forces is subject to similar principles.

We previously demonstrated the importance of accounting for mechanical and dynamic properties in the context of coarticulation in jaw movement kinematics during speech production (Ostry et al. 1996). Coarticulation is a phenomenon in which the articulator movements associated with a given speech sound vary systematically with the surrounding sounds and their associated movements. Although these variations may appear to be centrally planned, we showed, in the context of a mathematical model of jaw movement control that includes muscle mechanical properties and jaw dynamics (Laboissière et al. 1996), that even when central neural commands take no account of previous or upcoming context, kinematic patterns of jaw movements may nevertheless vary systematically in the same way as one observes empirically in demonstrations that suggest context sensitivity in speech production is centrally planned.

The present demonstration that the power law relation may arise as a consequence of muscle properties and limb dynamics cannot be taken as evidence that the power law relation is wholly unplanned. Although some aspects of the power law relation arise from biomechanical factors, others may be centrally planned. Schwartz (1994) has presented evidence that the power law is represented in motor cortical activity in monkeys during drawing tasks. Monkeys were trained to draw spiral patterns, during which activity of neurons in the motor cortex was recorded. The population vector method was used to transform the neuronal activity into a representation of the hand's trajectory. Schwartz (1994) showed that this cortical representation obeys the power law in portions of the trajectory where curvature was high (see also Pollick and Sapiro 1996). This suggests that the power law may indeed be a strategy at the level of central control. Moreover, as suggested by Viviani and Flash (1995), the power law relation may be a way to constrain the kinematic aspects of movements and reduce the available degrees of freedom of the system. The power law relation may thus reflect a combination of control along with aspects of muscle mechanics. This is consistent with recent proposals by Loeb et al. (1989) and Nichols (1994) that neural control and mechanics are matched.

Although the present simulations are based on the λ model, the present findings are not dependent on this particular model of control. As a demonstration of this, we have implemented the model of Flash (1987) of two joint planar arm movement which utilizes a model of control based on empirical measurements of joint stiffness and viscosity (see Flash 1987 for details). The parameter values were obtained from Flash (1987). As in the simulations reported above for the λ model, we used the Flash model to generate predicted hand paths based on elliptical equilibrium trajectories with constant tangential velocity. We found that the kinematics predicted with the use of Flash's model also conform to the power law, suggesting that the emergence of the power law is not dependent on our particular model of control, but

rather may arise as a result of the mechanics and dynamics of the limb.

As an additional illustration, we implemented a mathematical model of a simple two-dimensional mass-spring mechanical system and included no explicit model of control. In this model a mass was attached to two springs that apply forces to the mass along two orthogonal axes, X and Y, in the horizontal plane. The mass was displaced from the resting position in X and in Y, and the resulting simulated two-dimensional trajectory was measured. The tangential velocity and radius of curvature of the resulting trajectory were computed, and it was found that the simulated movement of the mass conformed to the power law relationship. In this case there was no explicit model of control—the mass was perturbed and the simulated movement that resulted was solely due to the mechanics of the system. This demonstration is consistent with the idea that the springlike properties of biomechanical systems such as the arm may contribute significantly to the emergence of the power law. Note that Lacquaniti et al. (1983) have also demonstrated that motion conforming to the power law can be produced by a system of coupled oscillators (see Wann et al. 1988 for a discussion of problems with using sinusoidal oscillators as models of movement control).

The authors acknowledge F. Pollick.

This research was supported by grants from the National Science and Engineering Research Council, Canada and the FCAR, Quebec.

Address for reprint requests: D. J. Ostry, Dept. of Psychology, McGill University, 1205 Dr. Penfield Ave., Montreal, Quebec H3A 1B1, Canada.

Received 15 April 1996; accepted in final form 22 July 1996.

REFERENCES

AN, K., HUI, F., MORREY, B., LINSCHEID, R., AND CHAO, E. Muscles across the elbow joint: a biomechanical analysis. *J. Biomech.* 14: 659–669, 1989a.

AN, K., KAUFMAN, K., AND CHAO, E. Physiological considerations of muscle force through the elbow joint. *J. Biomech.* 22: 1249–1256, 1989b.

FELDMAN, A. G. Once more on the equilibrium-point hypothesis (λ model) for motor control. *J. Mot. Behav.* 18: 17–54, 1986.

FELDMAN, A. G., ADAMOVICH, S. V., OSTRY, D. J., AND FLANAGAN, J. R. The origin of electromyograms—explanations based on the equilibrium point hypothesis. In: *Multiple Muscle Systems: Biomechanics and Movement Organization,* edited by J. Winters and S. Woo. New York: Springer-Verlag, 1990, p. 195–213.

FELDMAN, A. G. AND ORLOVSKY, G. N. The influence of different descending systems on the tonic reflex in the cat. *Exp. Neurol.* 37: 481–494, 1972.

FLASH, T. The control of hand equilibrium trajectories in multi-joint arm movements. *Biol. Cybern.* 57: 57–74, 1987.

HENNEMAN, E., SOMJEN, G., AND CARPENTER, D. O. Functional significance of cell size in spinal motoneurons. *J. Neurophysiol.* 28: 560–580, 1965.

HOLLERBACH, J. AND FLASH, T. Dynamic interactions between limb segments during planar arm movement. *Biol. Cybern.* 44: 67–77, 1982.

HOUK, J. AND RYMER, W. Neural control of muscle length and tension. In: *Handbook of Physiology. The Nervous System. Motor Control.* Bethesda, MD: Am. Physiol. Soc., 1981, sect. 1, vol. II, part 1, chapt. 8, p. 257–323.

HUXLEY, A. F. Muscle structure and theories of contraction. *Prog. Biophys. Chem.* 7: 255–318, 1957.

JOYCE, G. C. AND RACK, P. M. H. Isotonic lengthening and shortening movements of cat soleus muscle. *J. Physiol. Lond.* 204: 475–491, 1969.

LABOISSIÈRE, R., OSTRY, D., AND FELDMAN, A. The control of multi-muscle systems: human jaw and hyoid movements. *Biol. Cybern.* 74: 373–384, 1996.

LACQUANITI, F., TERZUOLO, C., AND VIVIANI, P. The law relating the kinematic and figural aspects of drawing movements. *Acta Psychol.* 54: 115–130, 1983.

LOEB, G., HE, J., AND LEVINE, W. Spinal cord circuits: are they mirrors of musculoskeletal mechanics? *J. Mot. Behav.* 21: 473–491, 1989.

MASSEY, J., LURITO, J., PELLIZZER, G., AND GEORGOPOULOS, A. Three-dimensional drawings in isometric conditions: relation between geometry and kinematics. *Exp. Brain Res.* 88: 685–690, 1992.

NICHOLS, T. A biomechanical perspective on spinal mechanisms of coordinated muscular action: an architecture principle. *Acta Anat.* 151: 1–13, 1994.

OSTRY, D., GRIBBLE, P., AND GRACCO, V. Coarticulation of jaw movements in speech production: is context sensitivity in speech kinematics centrally planned? *J. Neurosci.* 16: 1570–1579, 1996.

POLLICK, F. AND SAPIRO, G. Constant affine velocity predicts the 1/3 power law of planar motion perception and generation. *Vision Res.* In press.

SCHWARTZ, A. Direct cortical representation of drawing. *Science Wash. DC* 265: 540–542, 1994.

VIVIANI, P. AND CENZATO, M. Segmentation and coupling in complex movements. *J. Exp. Psychol. Hum. Percept. Perform.* 11: 828–845, 1985.

VIVIANI, P. AND FLASH, T. Minimum-jerk, two-thirds power law, and isochrony: converging approaches to movement planning. *J. Exp. Psychol. Hum. Percept. Perform.* 21: 32–53, 1995.

VIVIANI, P. AND SCHNEIDER, R. A developmental study of the relationship between geometry and kinematics in drawing movements. *J. Exp. Psychol. Hum. Percept. Perform.* 17: 198–218, 1991.

VIVIANI, P. AND STUCCHI, N. Biological movements look uniform: evidence of motor-perceptual interactions. *J. Exp. Psychol. Hum. Percept. Perform.* 18: 603–623, 1992.

WANN, J., NIMMO-SMITH, I., AND WING, A. Relation between velocity and curvature in movement: equivalence and divergence between a power law and a minimum-jerk model. *J. Exp. Psychol. Hum. Percept. Perform.* 14: 622–637, 1988.

WINTERS, J. AND WOO, S.-Y. (Editors). *Multiple Muscle Systems: Biomechanics and Movement Organization.* New York: Springer-Verlag, 1990.